

GLOBAL CORONAL SEISMOLOGY

I. BALLAI

Solar Physics and Space Plasma Research Centre (SP²RC), Department of Applied Mathematics, University of Sheffield, Hounsfield Road, Hicks Building, Sheffield, S3 7RH, U.K. (i.ballai@sheffield.ac.uk)

Received ; accepted

Abstract.

Following the observation and analysis of large-scale coronal wave-like disturbances, we discuss the theoretical progress made in the field of *global coronal seismology*. Using simple mathematical techniques we determine average values for magnetic field together with a magnetic map of the quiet Sun. The interaction between global coronal waves and coronal loops allows us to study loop oscillations in a much wider context, *i.e.* we connect global and local coronal oscillations.

Keywords: Sun: magnetic field, Sun: waves, Sun: coronal seismology

1. Introduction

The possibility of using waves propagating in solar atmospheric plasmas to infer quantities impossible to measure (magnetic field, transport coefficients, fine structuring, *etc.*) became a reality after high cadence observation of oscillatory motion was made possible by space and ground-based telescopes. These observations combined with theoretical models allow to develop a new branch of solar physics called *coronal seismology*. Pioneering studies by Uchida (1970), Roberts, Edwin and Benz (1984), Aschwanden *et al.* (1999) and Nakariakov *et al.* (1999), have formed the basis of a very promising and exciting field of solar physics.

Traditionally, the terminology of coronal seismology was used mainly to describe the techniques involving waves propagating in coronal loops. Since then, this word has acquired a much broader significance and the technique is generalised to acquire information about the magnetic solar atmosphere (De Pontieu, Erdélyi and James, 2004; Erdélyi, 2006). Coronal seismology uses waves which are localized to a particular magnetic structures, therefore it would be necessary to label these seismic studies as *local coronal seismology*. After the discovery of large-scale wave-like disturbances, such as EIT waves, X-ray waves, *etc.*, it became necessary to introduce a new terminology, *i.e.* *global coronal seismology* where the information is provided by global waves propagating over very large distances, sometimes comparable to the solar radius. Although this may seem a separate subject, in reality these



© 2018 Kluwer Academic Publishers. Printed in the Netherlands.

two aspects of coronal seismology are very much linked. A global wave generated by sudden energy releases (flares, CMEs) can interact with active region loops or prominences and localized loop or prominence waves and oscillations are emerging so, there must be a link between the generating source and flare-induced waves in coronal loops.

Global waves have been known since the early 1960s. Although it is still not known how the release of energy and energized particles will transform into waves, today it is widely accepted that these disturbances are similar to the circularly expanding bubble-like shocks after atomic bomb explosion or shock waves which follows the explosion of a supernova. Thanks to the available observational facilities, global waves were observed in a range of wavelengths in different layers of the solar atmosphere. A pressure pulse can generate seismic waves in the solar photosphere propagating with speeds of $200 - 300 \text{ km s}^{-1}$ (Kosovichev and Zharkova, 1998; Donea *et al.*, 2006). Higher up, a flare generates very fast super-alfvénic shock waves known as *Moreton waves* (Moreton and Ramsey, 1960), best seen in the wings of $H\alpha$ images, propagating with speeds of $1000 - 2000 \text{ km s}^{-1}$. In the corona, a flare or CME can generate an EIT wave (Thompson *et al.*, 1999) first seen by the SOHO/EIT instrument or an X-ray wave seen in SXT (Narukage *et al.*, 2002). There is still a vigorous debate how this variety of global waves are connected (if they are, at all). Co-spatial and co-temporal investigations of various global waves have been carried out but without a final widely accepted result being reached. The present study deals with the properties of EIT waves, therefore some characteristics of these waves will be given below.

Unambiguous evidence for large-scale coronal impulses initiated during the early stage of a flare and/or CME has been provided by the Extreme-ultraviolet Imaging Telescope (EIT) observations onboard SOHO and by TRACE/EUV. EIT waves propagate in the quiet Sun with speeds of $250 - 400 \text{ km s}^{-1}$ at an almost constant altitude. At a later stage in their propagation EIT waves can be considered a freely propagating wavefront which is observed to interact with coronal loops (see, *e.g.* Wills-Davey and Thompson, 1999). Using TRACE/EUV 195 Å observations, Ballai, Erdélyi and Pintér (2005) have shown that EIT waves (seen in this wavelength) are waves with average periods of the order of 400 seconds. Since at this height, the magnetic field can be considered vertical, EIT waves were interpreted as fast MHD waves.

2. Coronal Global EIT Waves and their Applications

The observations of EIT waves propagating in the solar corona allowed us to shed light on some elementary properties of coronal global EIT waves, however, the available observational precision does not permit us yet to determine more characteristics of these waves.

One of the un-answered problems related to EIT waves is connected to their propagation. The core of the problem resides in the lack of detection of an EIT wave with every flare or CME. This could be explained partly by the poor temporal resolution of the SOHO satellite (the only satellite giving full-disk EUV images at the moment) where frames are available with a low cadence, therefore EIT waves generated near the limb simply cannot be recorded. In general, EIT waves seen by SOHO are generated by sources which are located near the centre of the solar disk. EUV images provided by TRACE are much better to use, although the field of view of this instrument is limited. Since EIT waves propagate over a large area of the solar surface (at a certain altitude) they are dispersive. Other ingredients to be considered are the stratification of the medium and the inhomogeneous character of the plasma. All of these factors influence the propagation of coronal EIT waves.

Another plausible explanation for the absence of EIT waves associated with every flare or CME might be that EIT waves diffuse very rapidly, *i.e.* they become evanescent in a short time after their launch. This means that only those EIT waves could be observed which propagate as guided (trapped) waves. The MHD equations in a gravitationally-stratified plasma allows as a solution the magnetoacoustic/magnetogravitational waves of growing amplitude with time (upward propagating waves) and decreasing amplitude with time (downward propagating waves). Trapped EIT waves might arise as a combination of magnetoacoustic and magnetogravitational waves propagating in opposite directions. Further investigations of the possibility of trapping spherical waves in a dissipative medium are needed.

2.1. INTERACTION OF EIT WAVES WITH OTHER CORONAL MAGNETIC ENTITIES

In this subsection we enumerate a few possible phenomena arising from the interaction of global EIT waves with coronal magnetic entities. According to the classical picture, EIT waves collide with coronal loops resulting in a multitude of modes generated in loops either in the form of standing oscillations or propagating waves. Both types of waves have the general property that they decay very rapidly in a few wavelengths

or periods (see *e.g.* Nakariakov *et al.*, 1999; Aschwanden *et al.*, 2002). This damping was later used to diagnose the magnetic field inside coronal loops (Nakariakov *et al.*, 1999), transport coefficients for slow waves or global fast waves, sub-structuring, heating function, *etc.*

In coronal loops we consider only the transversal generation of waves, *i.e.* waves and oscillations are triggered by the interaction of EIT waves and coronal loops. From the EIT wave point of view, a coronal loop (similar to an active region or coronal hole) is an entity with a stronger magnetic field (at least one order of magnitude) than the medium in which they propagate (quite Sun). Therefore, beside transferring energy to coronal loops, EIT waves can be scattered, reflected, and refracted (Terradas and Ofman, 2004). Without claiming completeness, we can draw a few conditions that could influence the appearance of coronal loop oscillations:

- *height of the loop*: since EIT waves propagate at certain heights in the solar corona, it is likely that not all loops will interact with the global waves. Schrijver, Aschwanden and Title (2002) pointed out that only those loops will be affected by EIT waves whose heights exceed 60 – 150 Mm. This means that cool, low-lying loops will not interact with EIT waves.

- *the height of the interaction between EIT waves and coronal loops*: this factor simply means that it is easier to generate oscillations in a loop if the interaction point between the EIT wave and coronal loop is closer to the apex of the loop rather than the footpoint.

- *Orientation of the loop*: if the front of the EIT wave is perpendicular to the plane of the coronal loop the interaction between the EIT waves and the coronal loop occurs in two points at the same time. If the loop is stiff enough, a standing oscillation can be easily excited. If the front is not perpendicular, the collision between the EIT wave and loops occurs in two points delayed in time by $\tau = s \cos \alpha / v_{EIT}$, where s is the distance between the footpoints, α is the attack angle, and v_{EIT} is the propagation speed of the EIT wave. In this case, standing modes can be excited only in very special cases. Another important element is the orientation of the coronal loop with respect to the vertical axis (inclination).

- *distance between the flaring site and coronal loop* (or energy of EIT waves): During their propagation, EIT waves are losing energy due to the geometrical damping (dilatation of the front) and due to some physical damping effects. Therefore it might happen that the energy of an EIT wave originating from a distant flare is not enough to dislocate the loop.

- *radius of the loop and the density contrast* (or Alfvén speed contrast): a massive loop is much harder to dislocate than a thin loop. The ratio

between the densities in the loop and its environment is known to influence the amplitude of oscillations.

In order to describe quantitatively the interaction between EIT waves and coronal loops, we suppose a medium in which the coronal loop is situated, for simplicity, in a magnetic-free medium (in fact this constraint can be relaxed and the result is obvious) retains its identity and does not disperse or fragment. The tube is considered thin, *i.e.* its radius is small relative to other geometrical scales of the problem. During the wave propagation we suppose a quasi-static pressure balance to be maintained at all times.

An EIT wave colliding with a coronal loop exerts a force which will need to work against two forces, one being the elastic force of the tube represented by the magnetic tension of the tube and inertia of the fluid element which needs to be displaced.

The equilibrium of the tube is prescribed by the hydrostatic equilibrium where pressure forces are in equilibrium with the gravitational force and the lateral pressure balance $p_i + B_i^2/2\mu = p_e$ is satisfied, with p_i and p_e being the kinetic (thermal) pressure inside the tube and the environment, B_i the interior magnetic field and g is the gravitational acceleration at the solar surface. If we denote by ρ_i and ρ_e the locally homogeneous densities inside and outside the tube and $v_A (= B_i/(\mu\rho_i)^{1/2})$ the Alfvén speed, then the equation describing the variation of displacement of the fluid element, $\xi(z, t)$, is (a similar equation has been obtained by Ryutov and Ryutova (1975) in a different context)

$$\frac{\partial^2 \xi}{\partial t^2} = -g \frac{\rho_i - \rho_e}{\rho_i + \rho_e} \frac{\partial \xi}{\partial z} + \frac{\rho_i}{\rho_i + \rho_e} v_A^2 \frac{\partial^2 \xi}{\partial z^2}. \quad (1)$$

Let us introduce a new variable such that $\xi(z, t) = Q(z, t) \exp(\lambda z)$, where the value of λ is chosen such that the first-order derivatives with respect to the coordinate z vanish. After a straightforward calculation we obtain that the dynamics of generated waves in the coronal loop as a result of the interaction of a global wave with coronal loop is described by

$$\frac{\partial^2 Q}{\partial t^2} - c_K^2 \frac{\partial^2 Q}{\partial z^2} + \omega_C^2 Q = 0, \quad \omega_C = \frac{g(d-1)}{2v_A \sqrt{d(d+1)}},$$

$$c_K = v_A \left(\frac{d}{1+d} \right)^{1/2} \quad (2)$$

with $d = \rho_i/\rho_e$ being the filling factor. Equation (2) is the well-known Klein-Gordon (KG) equation derived and studied earlier in solar MHD wave context by, *e.g.* Rae and Roberts (1982), Hargreaves (2005), Ballai, Erdélyi and Hargreaves (2006). The quantity c_K is the kink speed

of waves and it is regarded as a density-weighted Alfvén speed. The coefficient ω_C is the cut-off frequency of waves and is a constant quantity for an isothermal medium.

The waves corresponding to the Eq. (2) are dispersive, *i.e.* waves with smaller wavelength (larger k) propagating faster. Waves with smaller wave number will have smaller group speed, the maximum of the group speed (at $k \rightarrow \infty$) being c_K . Another essential property of the KG equation is that it describes waves which are able to propagate if their frequency is larger than the cut-off frequency. For typical coronal conditions ($v_A=1000$ km s⁻¹, $d = 10$) we obtain that waves will propagate if their frequency is greater than 0.11 mHz or their period is smaller than 150 minutes.

For simplicity, let us suppose that the fast kink mode in the coronal loop is generated by the interaction of an EIT wave with a loop and the forcing term of the interaction is modelled by a delta-pulse, *i.e.* the equation describing the dynamics of impulsively generated fast kink mode is given by

$$\frac{\partial^2 Q}{\partial t^2} - c_K^2 \frac{\partial^2 Q}{\partial z^2} + \omega_C^2 Q = \delta(z)\delta(t). \quad (3)$$

This equation can be solved using standard Laplace transform technique to yield

$$Q(z, t) = \frac{c_K}{2} J_0 \left(\omega_C \sqrt{c_K^2 t^2 - z^2} \right) H(c_K t - |z|), \quad (4)$$

where $J_0(z)$ is the zeroth-order Bessel function and $H(z)$ is the Heaviside function. The impulsive excitation of waves in a flux tube leads to the formation of a pulse that propagates away with the speed c_K , followed by a wake in which the flux tube oscillates with the frequency ω_C . A typical temporal variation of the amplitude of kink waves (keeping the height constant) would show that the amplitude of the mode decreases (even in the absence of dissipation) and an e-fold decay occurs in about 400 seconds .

Recently Terradas, Oliver and Ballester (2005) have studied the interaction between the coronal loops and EIT waves in the zero-beta limit considering a spatial initial condition. They obtained that the generated oscillations in the coronal loop decay asymptotically as $t^{-1/2}$. Kink oscillations are weakly affected by dissipation, therefore the consideration of any non-ideal effect to supplement the KG equation would not lead to a significant change. It is accepted that damping due to the resonant absorption could explain the damping of kink oscillations in coronal loops (Ruderman and Roberts, 2002; Goossens, Andries and Aschwanden, 2002).

It can be shown that the consideration of resonant absorption as a damping mechanism in the governing equation leads to a similar equation we would obtain taking into account dissipation. Ballai, Erdélyi and Hargreaves (2006) showed that the evolution equation is modified by an extra term forming a Klein-Gordon-Burgers (KGB) equation

$$\frac{\partial^2 Q}{\partial t^2} - c_K^2 \frac{\partial^2 Q}{\partial z^2} + \omega_C^2 Q - \nu \frac{\partial^3 Q}{\partial z^2 \partial t} = 0, \quad (5)$$

where ν is a coefficient which could play the role of any dissipative mechanism or a factor which include the damping due to resonant absorption (in fact ν is inversely proportional to the gradient of Alfvén speed) and would describe the transfer of energy from large to small scales (see, *e.g.* Ruderman and Goossens, 1993).

Waves in this approximation can have a temporal (keeping k real) and spatial damping (keeping ω real), the decay rate and length, supposing the ansatz $Q(z, t) \sim \exp[i(\omega t - kz)]$, are given by

$$\omega_i = \frac{i\nu k^2}{2}, \quad k_i \approx -\frac{\nu\omega}{2c_K} \sqrt{\frac{\omega^2 - \omega_C^2}{c_K^4 + \nu^2\omega^2}}. \quad (6)$$

The KGB equation can be solved using initial/boundary conditions to describe the evolution of kink modes for different kind of sources, *e.g.* monochromatic source ($A(t) = V_0 e^{i\Omega t}$), delta-function pulse ($A(t) = V_0 \delta(\omega_C t / 2\pi)$), *etc.* using numerical methods. Asymptotic analysis ($t \gg z/c_K$) shows that these waves decay as $t^{-3/2}$ (Ballai, Erdélyi and Hargreaves, 2006).

Another important factor is the energy of EIT waves. Recently Ballai, Erdélyi and Pintér (2005), using a simple energy conservation, found the minimum energy an EIT wave should have to produce a loop oscillation. Using their results we studied a few loop oscillation events presented by Aschwanden *et al.* (2002) and the minimum energy of EIT waves necessary to produce the observed oscillations are shown in Table 1. The geometrical size of loops and the number densities given by Aschwanden *et al.* (2002) have been used.

The obtained energies are in the range of $10^{16} - 10^{19}$ J with no particular correlation with the length and radius of the loop. Similar to this approach we can estimate the minimum energy of an EIT wave to produce a displacement of 1 pixel in TRACE/EUV 195 Å images using the relation $E = 1.66 \times 10^6 L (\rho_i R^2 + \rho_e / \lambda_e^2)$, (J) where L and R are the length and radius of the loop, and λ_e^{-1} the decay length of perturbations outside the cylinder given by

$$\lambda_e^2 = \frac{(c_{Se}^2 - c_K^2)(v_{Ae}^2 - c_K^2)}{(c_{Se}^2 + v_{Ae}^2)(c_{Te}^2 - c_K^2)} k^2, \quad (7)$$

Table I. The minimum energy of EIT waves which could produce the loop oscillations studied by Aschwanden *et al.* (2002).

Date(yyymmdd)	L(Mm)	R(Mm)	$n(\times 10^8 \text{ cm}^{-3})$	E(J)
1998 Jul 14	168	7.2	5.7	2.2×10^{17}
1998 Jul 14	204	7.9	6.2	9.7×10^{18}
1998 Nov 23	190	16.8	3	1.3×10^{19}
1999 Jul 04	258	7	6.3	3.9×10^{16}
1999 Oct 25	166	6.3	7.2	1.6×10^{18}
2000 Mar 23	198	8.8	17	5.2×10^{16}
2000 Apr 12	78	6.8	6.9	2.5×10^{16}
2001 Mar 21	406	9.2	6.2	7.4×10^{16}
2001 Mar 22	260	6.2	3.2	1.9×10^{16}
2001 Apr 12	226	7	4.4	1.4×10^{18}
2001 Apr 15	256	8.5	5.1	1.4×10^{16}
2001 May 13	182	11.4	4	2.2×10^{18}
2001 May 15	192	6.9	2.7	1.6×10^{19}
2001 Jun 15	146	15.8	3.2	1.1×10^{17}

with c_{Te} , c_{Se} , and v_{Ae} being the cusp, sound and, Alfvén speeds in the region outside the loop and k is the wavenumber. The energy range is in the interval $3 \times 10^{17} - 3 \times 10^{18}$ J for loop lengths and radii varying in the intervals 60–500 Mm and 1–10 Mm.

2.2. DETERMINATION OF MAGNETIC FIELD VALUES

Observations show that EIT waves propagate in every direction almost isotropically on the solar disk, therefore we can reasonably suppose that they are fast magnetoacoustic waves (FMWs) propagating in the quiet Sun perpendicular to the vertical equilibrium magnetic field. The representative intermediate line formation temperature corresponding to the 195 Å wavelength is 1.4×10^6 K. The sound speed corresponding to this temperature is 179 km s^{-1} . Since the FMWs propagate perpendicular to the field, their phase speed is approximated by $(c_S^2 + v_A^2)^{1/2}$.

The propagation height is an important parameter as a series of physical quantities (density, temperature, *etc.*) in the solar atmosphere have a height dependence. Given the present status of research on the propagation of EIT waves, there is no accepted value for the propagation height of these waves. For a range of the plasma parameters we can derive average values for the magnetic field by considering the propagational characters of EIT waves. Therefore, we study the

variation of various physical quantities with respect to the propagation height of EIT waves.

We recall a simple atmospheric model developed by Sturrock, Wheatland and Acton (1996). The temperature profile above a region of the quiet Sun, where the magnetic field is radial, is given by

$$T(x) = \left[T_0^{7/2} + \frac{7R_\odot F_0}{2a} \left(1 - \frac{1}{x} \right) \right]^{2/7}. \quad (8)$$

Here F_0 is the inward heat flux (1.8×10^5 erg cm $^{-2}$ s $^{-1}$), x is the normalized height coordinate defined by $x = r/R_\odot$, T_0 is the temperature at the base of the model (considered to be 1.3×10^6 K) and a is the coefficient of thermal conductivity. The quantity a is weakly dependent on pressure and atmospheric composition; for the solar corona a value of 10^{-6} (in cgs units) is appropriate (Nowak and Ulmschneider, 1977). Assuming a model atmosphere in hydrostatic equilibrium we obtain that the number density, based on the temperature profile supposed in Eq. (8), is

$$n(x) = \frac{n_0 T_0}{T(x)} \exp[-\delta(T(x)^{5/2} - T_0^{5/2})], \quad \delta = \frac{2\mu G M_\odot m_p a}{5k_B R_\odot^2 F_0}, \quad (9)$$

with G the gravitational constant, M_\odot the solar mass, k_B is the Boltzmann's constant; $\mu = 0.6$ is the mean molecular weight; m_p , proton mass and $n_0 = 3.6 \times 10^8$ cm $^{-3}$ the density at the base of corona. Having the variation of density with height and the value of Alfvén speed deduced from the phase speed of EIT waves, we can calculate the magnetic field using $B = v_A(4\pi m_p n)^{1/2}$. Evaluating the relations above, the variation of temperature, density, Alfvén speed and magnetic field with height is shown in Table 2. Two cases are derived for EIT waves propagating strictly perpendicular to the radial magnetic field with a speed of (a) 250 km s $^{-1}$ and, (b) 400 km s $^{-1}$, respectively. The values of the physical quantities show some change for a given propagation speed but will have little effect on the final results.

For an average value of EIT wave speed of 300 km s $^{-1}$ propagating at $0.05 R_\odot$ above the photosphere we find that the magnetic field is 1.8 G. If we apply $Br^2 = const.$, *i.e.* the magnetic flux is constant, we find that at the photospheric level the average magnetic field is 2.1 G which agrees well with the observed solar mean magnetic field (Chaplin *et al.* 2003). EIT waves considered as fast MHD waves can also be used to determine the value of the radial component of the magnetic field at every location allowed by the observational precision. In this way, using the previously cited TRACE observations we can construct a magnetic map of the quiet Sun (see Figure 1), in other words EIT

Table II. The variation of the temperature (in MK), density (in units of 10^8 cm^{-3}), Alfvén and sound speeds (in units of 10^7 cm s^{-1}) and magnetic field (in G) with height above the photosphere for an EIT wave propagating with a speed of (a) 250 km s^{-1} , and (b) 400 km s^{-1} , respectively.

r/R_\odot	T	n	c_S	$v_A^{(a)}$	$B^{(a)}$	$v_A^{(b)}$	$B^{(b)}$
1.00	1.30	3.60	1.72	1.81	1.57	3.61	3.13
1.02	1.41	3.30	1.80	1.73	1.44	3.57	2.97
1.04	1.50	3.10	1.85	1.67	1.34	3.54	2.85
1.06	1.58	2.95	1.90	1.61	1.27	3.51	2.76
1.08	1.64	2.83	1.94	1.57	1.21	3.49	2.69
1.10	1.70	2.73	1.97	1.52	1.15	3.47	2.63

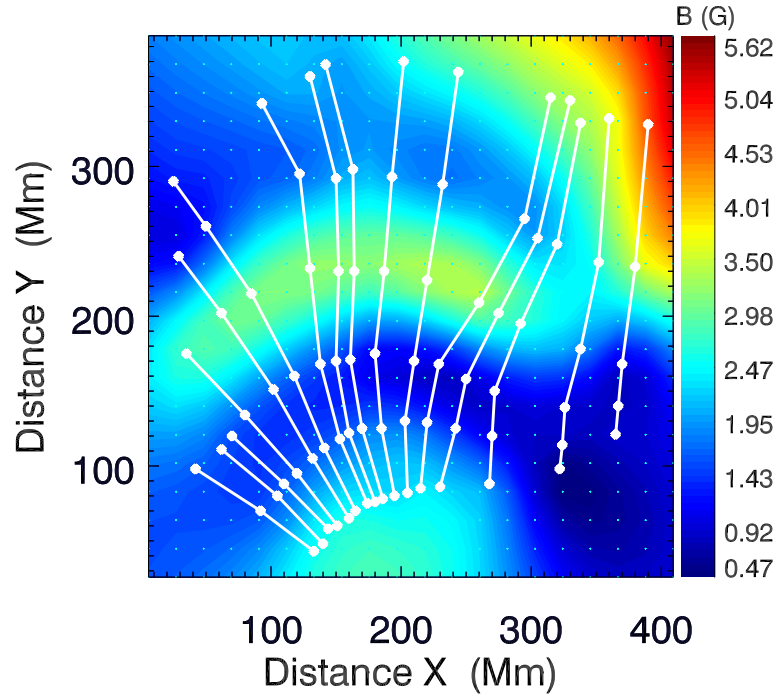


Figure 1. Magnetic map of the quiet Sun obtained using an EIT wave observed by TRACE/EUV in 195 \AA .

waves can serve as probes in a *magnetic tomography* of the quiet Sun. If points are joined across the lines, we will obtain the location of the EIT wavefront. Magnetic field varies between 0.47 and 5.62 G, however, these particular values should be handled with care as the interpolation will introduce spurious values at the two ends of the interval. It should be noted that this result has been obtained supposing a single value for density, in reality both magnetic field and density can vary along the propagation direction, as well. The method we employed to find this magnetic map (magnetic field derived via the Alfvén speed) means that density and magnetic field cannot be determined at the same time. Further EUV density sensitive diagnostics line ratio measurements are required to establish a density map of the quiet Sun which will provide an accurate determination of the local magnetic field.

In conclusion, EIT waves propagating in the solar corona exhibit a wide range of applicabilities for plasma and field diagnostics. The fact that during their propagation EIT waves cover a large area of the solar surface (in the coronal) allows us to sample the magnetic field in the quiet Sun. EIT waves could serve as a link between eruptive events and localised oscillations, *e.g.* loop oscillations could be studied in a much broader context. Using a simple model we found that the minimum energy an EIT wave should have to produce a detectable loop oscillation is in the range of $10^{16} - 10^{19}$ J.

Problems to be tackled in the future should include the study of attenuation of EIT waves with the aim of providing information about the magnitude of transport coefficients in the quiet Sun. The old problem of connecting different global waves still remain to be addressed.

Despite of the lack of high precision observations, EIT waves show a great potential for magneto-seismology of the solar corona.

Acknowledgements

The author acknowledges the financial support offered by the Nuffield Foundation (NUF-NAL 04) and NFS Hungary (OTKA, T043741). The help by B. Pintér and M. Douglas is appreciated.

References

- Aschwanden, M.J., Fletcher, L., Schrijver, C.J., Alexander, D.: 1999, *Astrophys. J.*, **520**, 880
 Aschwanden, M.J., De Pontieu, B., Schrijver, C.J., Title, A.M.: 2002, *Solar Phys.*, **206**, 99
 Ballai, I., Erdélyi, R., Pintér, B.: 2005, *Astrophys. J.* **633**, L145

- Ballai, I., Erdélyi, R., Hargreaves, J.: 2006, *Phys. Plasmas*, **13**, 042108
- Chaplin, W.J., Dumbhill, A.H., Elsworth, Y., Isaak, G.R., McLeod, C.P. *et al.*: 2003, *Mon. Not. Roy. Astron. Soc.* **343**, 813
- De Pontieu, B., Erdélyi, R., James, S.: 2004, *Nature*, **430**, 536
- Donea, A.-C., Besliu-Ionescu, D., Cally, P., Lindsey, C., Zharkova, V.V.: 2006, *Solar Phys.*, **239**, 113
- Erdélyi, R.: 2006, *Proc. Roy. Soc. London Ser. A*, **364**, 351
- Goossens, M., Andries, J., Aschwanden, M.J.: 2002, *Astron. Astrophys.*, **394**, 39
- Hargreaves, J.: 2005, in Ballai *et al.* (eds.) *Plasma- and Astrophysics: from laboratory to outer space*, *PADEU*, **15**, 83
- Kosovichev, A.G., Zharkova, V.: 1998, *Nature*, **393**, 317
- Moreton, G.F., Ramsey, H.E.: 1960, *Publ. Astron. Soc. Pac.*, **72**, 357
- Nakariakov, V.M., Ofman, L., DeLuca, E.D., Roberts, B., Davila, J.M.: 1999, *Science*, **285**, 862
- Narukage, N., Hudson, H.S., Morimoto, T., Akiyama, S., Kitai, R. *et al.*: 2002, *Astrophys. J.*, **572**, L109
- Nowak, T., Ulmschneider, P.: 1977, *Astron. Astrophys.*, **60**, 413
- Rae, I.C., Roberts, B.: 1982, *Astrophys. J.*, **256**, 761
- Roberts, B., Edwin, P.M., Benz, A.O.: 1984, *Astrophys. J.*, **279**, 857
- Ruderman, M.S., Goossens, M.: 1993, *Solar Phys.*, **143**, 69
- Ruderman, M.S., Roberts, B.: 2002, *Astrophys. J.*, **577**, 475
- Ryutov, D.A., Ryutova, M.P.: 1975, *JETP*, **43**, 491
- Schrijver, C.J., Aschwanden, M.J., Title, A.M.: 2002, *Solar Phys.*, **206**, 69
- Sturrock, P., Wheatland, M.S., Acton, L.: 1996, *Astrophys. J.*, **461**, L115
- Terradas, J., Ofman, L.: 2004, In Erdélyi, Ballester and Fleck (eds.) *SOHO 13: Waves, Oscillations and Small-Scale Transient Events in the Solar Atmosphere*, **ESA SP-547**, Noordwijk, ESA, 469
- Terradas, J., Oliver, R., Ballester, J.L.: 2005, *Astrophys. J.*, **618**, L149
- Thompson, B.J., Gurman, J.B., Neupert, W.M. *et al.*: 1999, *Astrophys. J.*, **517**, 151
- Uchida, Y.: 1970, *Publ. Astron. Soc. Pac.*, **22**, 341
- Wills-Davey, M.J., Thompson, B.J.: 1999, *Solar Phys.*, **190**, 467